Supporting information for

Ultrahigh-surface-area nitrogen-doped hierarchically porous carbon materials derived from chitosan and betaine hydrochloride sustainable precursors for high-performance supercapacitors

Jian Cheng‡, Qinqin Xu‡, Xia Wang, Zaiquan Li, Fuzhong Wu,* Jiaojing Shao, Haibo Xie*

Department of New Energy Science & Engineering,

The Key Laboratory of Metallurgical Engineering and Process Energy Saving,

College of Materials and Metallurgy, Guizhou University, Guiyang 550025, P.R.China

Corresponding Authors: Email: gutwfz@163.com; hbxie@gzu.edu.cn

S1. Electrochemical measurements

The gravimetric (C_g, F g^{-1}) of a single electrode was calculated from the discharge curves according to the following equations(1-2) [1-4]:

$$C_{g=}\frac{2I \bigtriangleup t}{m \bigtriangleup V} \tag{1}$$

where I (A) is the constant discharge current, Δt (s) is the discharge time, m (g) is the mass of the active material in a single electrode, ΔV (V) is the voltage change in discharge.

The gravimetric energy density (W_g,Wh kg^{-1}) and power density (P_g, W kg^{-1}) of the two-electrode symmetric supercapacitors were also calculated according to equation (2 – 3):

$$W_g = \frac{C_g \Delta V^2}{8x3.6} \tag{2}$$

$$P_g = \frac{3600xWg}{\Delta t} \tag{3}$$

where C_g (F g^{-1}) represents the gravimetric specific capacitance of a single electrode obtained from equation (1), ΔV (V) is the voltage change in discharge, Δt (s) is the discharge time.

S2. SScheme & SFigures & STables

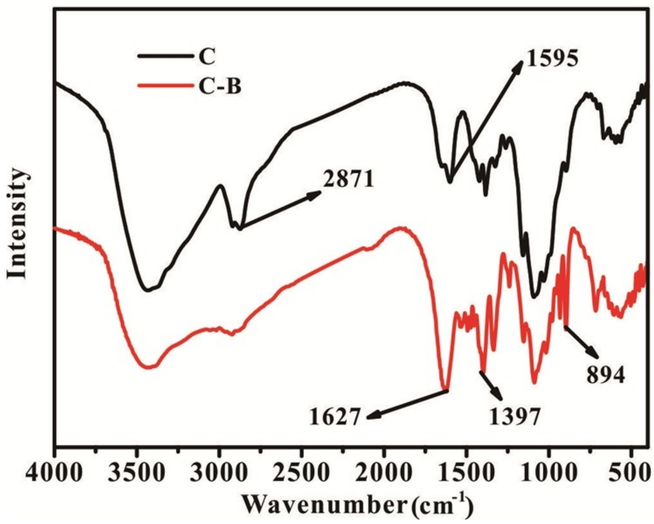

Figure S1. Comparative FT-IR spectra of Chitosan (C) and CBHP (C-B)

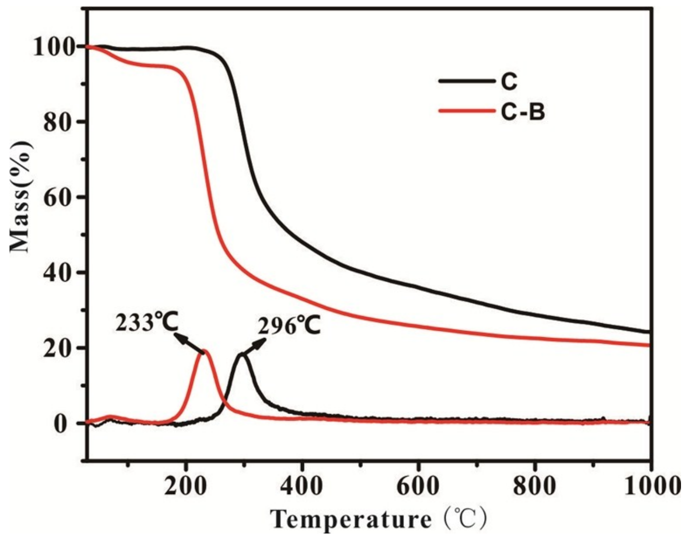

Figure S2. Thermogravimetric analysis (TGA) of chitosan: C and CBHP

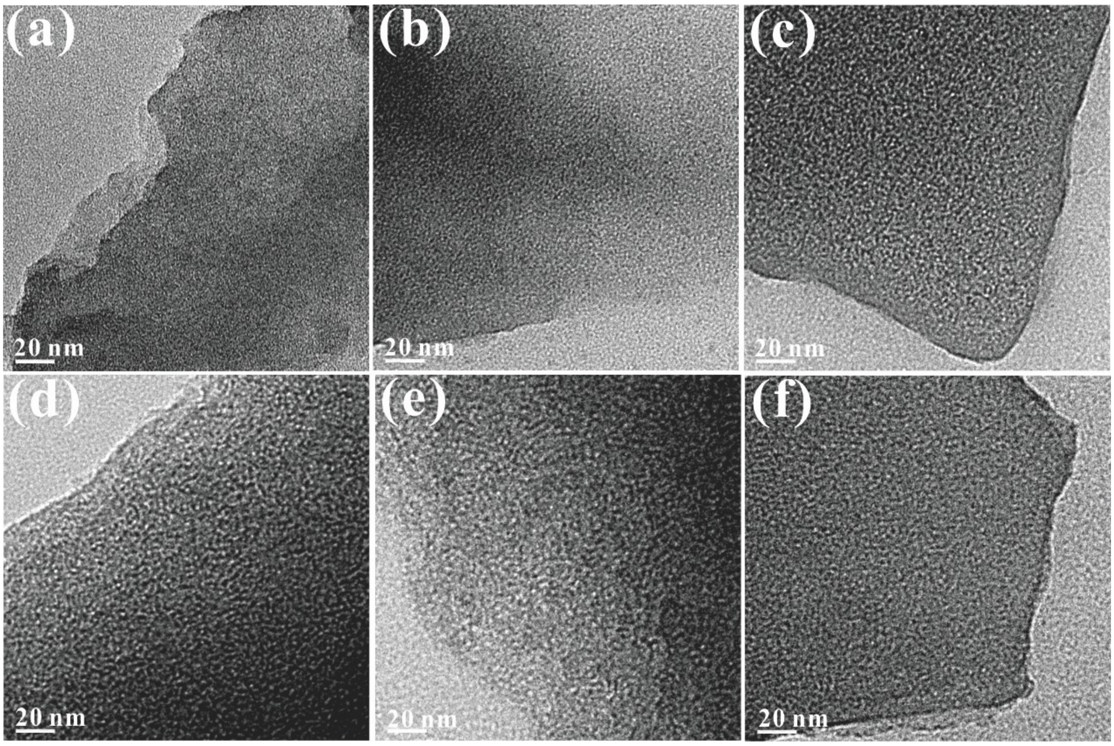

Figure S3. TEM images of C-B-X-Y carbon materials: (a) C-B-800; (b)C-B-KOH-300; (c) C-B-KOH-400; (d) C-B-KOH-500; (e) C-B-K_2FeO_4-400; (f) C-B-KCl-800.

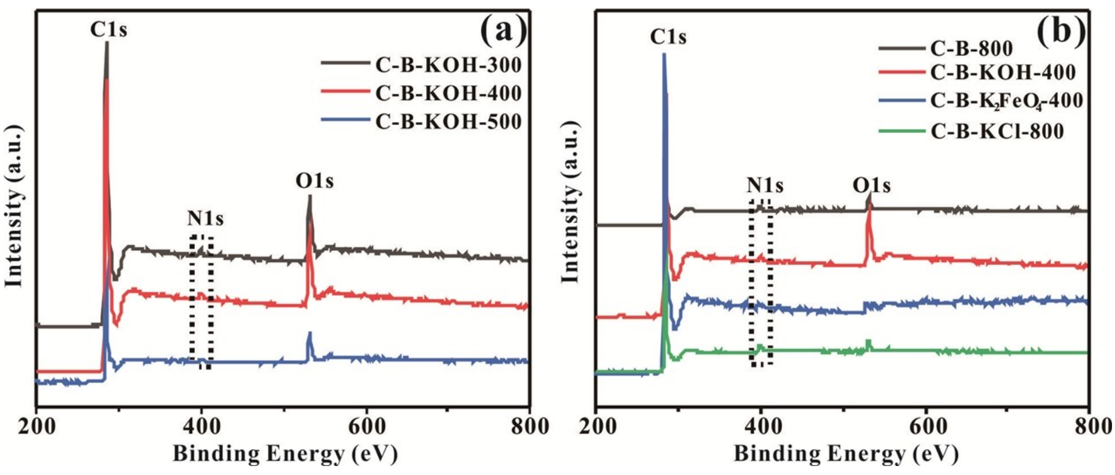

Figure S4. XPS survey spectra of (a) C-B-KOH-Y(300℃-500℃) and (b) C-B-X-Y.

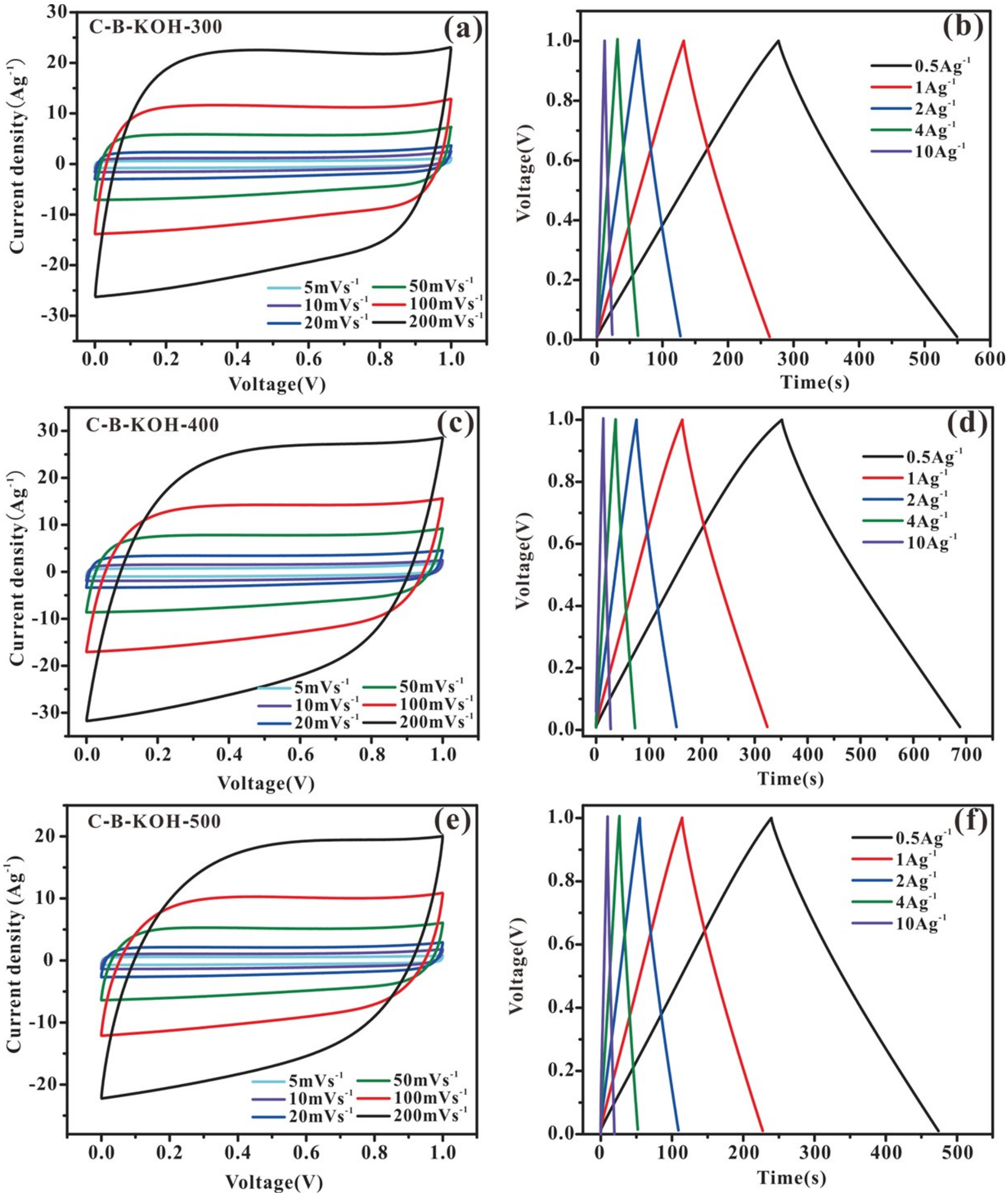

Figure S5. Cyclic voltammetry at 20 mVs^{-1} ~ 200 mVs^{-1} and GCD curves at 0.5 Ag^{-1} ~ 10Ag^{-1} of C-B-KOH-Y (300℃ ~ 500℃) in 6 molL^{-1} KOH .

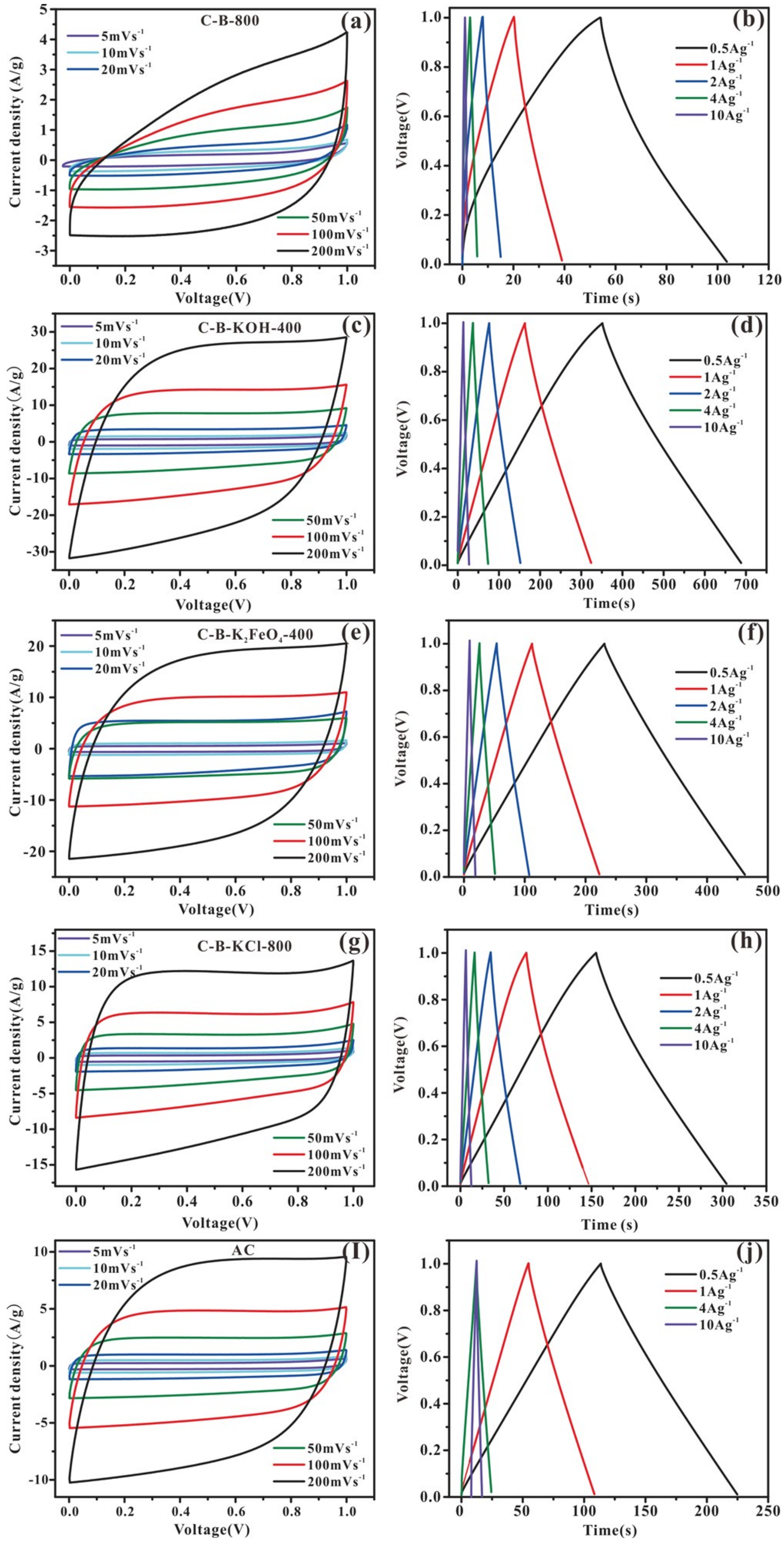

Figure S6. Cyclic voltammetry at 20 mVs^{-1} ~ 200 mVs^{-1} and GCD curves at 0.5 Ag^{-1} ~10 Ag^{-1} of C-B-X-Y in 6 $molL^{-1}$ KOH

Table S1 Adsorption parameters from N_2 adsorption isotherms and electrochemical performances of the as-prepared N-doped carbon material samples.

Sample	BET surface area[a] ($m^2\ g^{-1}$)	Total pore volume[b] ($cm^3\ g^{-1}$)	Micropore volume[c] ($cm^3\ g^{-1}$)	Most probable pore[d] diameter (nm)	C_g[e] ($F\ g^{-1}$)
C-B-800	81	0.24	0.003	12.31	90
C-B-KOH-300	2780	1.35	0.61	1.9	302
C-B-KOH-400	3331	2.24	0.87	2.28	367
C-B-KOH-500	2438	1.22	0.81	1.77	260
C-B-KCl-800	510	0.82	0.39	3.48	168
C-B-K_2FeO_4-400	1815	0.99	0.47	2.18	253

a: Surface area (BET) calculated using the BET method.

b: Total pore volume determined at a relative pressure (P/P_0) of 0.99.

c: Micropore volume calculated using the DFT model.

d: Pore size distribution is calculated by using the NLDFT method.

e: The C_g values calculated from discharge curves at a current density of 0.1 A g^{-1} in 6 M KOH.

Table S2 Comparison of the specific surface area (S_{BET}) performance in this work and other literatures

Materials	Activation Method	Activation Agent	S_{BET} (m^2 g^{-1})	Refs
Chitosan	**Chemical**	**KOH**	**3330**	**This work**
		K_2FeO_4	**1815**	
Chitosan	Chemical	K_2CO_3	1013	[5]
Chitosan	Chemical	KOH	2435	[6]
Chitosan	Chemical	KOH	2616	[7]
Chitosan	Chemical	$ZnCl_2$	1582	[8]
Chitosan	Chemical	$ZnCl_2$	1567	[9]
Chitosan	Physical	CO_2	1054	[10]
Chitosan	Chemical	$ZnCl_2$	1785	[11]
Chitosan	Chemical	Na_2CO_3	440	[12]
Chitosan	Chemical	$Zn(NO_3)_2 \cdot 6H_2O$	1956	[13]
Chitosan	Chemical	KOH	2169	[14]
Chitosan	Chemical	KOH	2807	[15]
Chitosan	Chemical	KOH	2397	[15]
Starch	Chemical	KOH	2273	[16]
Pumpkin	Chemical	KOH	2968	[17]
Peanut shell	Chemical	KOH	2396	[18]
Paulownia sawdust	Chemical	NaOH	1962	[19]
Lignin	Chemical	KOH	2218	[20]
Sawdust	Chemical	KOH	1850	[21]
Glucose	Chemical	$ZnCl_2$+KCl	2160	[22]
Wheat straw	Chemical	KOH	2316	[23]
Cherry stones	Chemical	KOH	1273	[24]
Waste news paper	Chemical	KOH	416	[25]
Hemp bast fiber	Chemical	KOH	2287	[26]
Spider silk	Chemical	$ZnCl_2$	721	[27]
Broussonetia papyrifera	Chemical	KOH	1212	[28]
Neem dead leaves	Chemical	KOH	1230	[29]
Black liquor	Chemical	KOH	2646	[30]

Table S3 Comparison of the supercapacitances performance in this work and other literatures

Materials	Capacitance (F/g)	Current density (A g^{-1})	Electrolyte	Max energy density (Wh/kg)	Max power density (w/kg)	Voltage Window(V)	Refs
Activated carbon	195	0.5	6 M KOH	10	1000	1	[31]
Mesoporous Carbon	227	0.2	6 M KOH			1	[32]
Hierarchical Porous Carbon	139	1	1 M $LiPF_6$	37.9	700	2.8	[33]
hierarchical porous carbons	336	1	6 M KOH	72.7	1204	2.5	[34]
Hierarchically Porous Carbon	253	0.5	6 M KOH			1	[35]
Nano Porous Active Carbon	225	0.5	6 M KOH	7.8	250	1	[36]
Microporous Carbon	286.1	1	6 M KOH	53.6	1124.5	1.5	[37]
hierarchical porous carbon	309	0.5	1 M H2SO4	10.7	125	1	[38]
Biomass-Derived Carbon	225	0.5	$NaClO_4$ in EC/DMC	70	375	3	[39]
Hollow carbon microtube	121	1	6 M KOH	35	750	1.5	[40]
Renewable Carbon	215	0.1	6 M KOH			0.8	[41]
Hierarchical Porous Carbons	217.7	1	ionic liquid $BMIMBF_4$	92.6	879.6	3.5	[42]
Hierarchical porous carbon nanosheets	350	0.1	6 M KOH	12.2	25.0	1.5	[43]
Porous carbon nanosheets	275	0.5	6 M KOH	7.8	250	1	[44]
Microporous carbon nanocomposites	237	0.1	3 M H_2SO_4			0.9	[45]
Mesoporous carbons	312	1	6 M KOH	9.2	23	1	[46]
graphene nanosheets	201	0.05	1 M H_2SO_4	6.2	25	1	[47]

3. References

[1]. Lang, J.-w., et al., *Influence of nitric acid modification of ordered mesoporous carbon materials on their capacitive performances in different aqueous electrolytes.* J. Power Sources, 2012. **204**: p. 220-229.

[2]. Sun, L., et al., *From coconut shell to porous graphene-like nanosheets for high-power supercapacitors.* J. Mater Chem. A, 2013. **1**(21): p. 6462-6470.

[3]. Wang, G., et al., *Preparation and supercapacitance of CuO nanosheet arrays grown on nickel foam.* J. Power Sources, 2011. **196**(13): p. 5756-5760.

[4]. Jha, N., et al., *High Energy Density Supercapacitor Based on a Hybrid Carbon Nanotube–Reduced Graphite Oxide Architecture.* ADV ENERGY MATER, 2012. **2**(4): p. 438-444.

[5]. Zhang, F., et al., *Hierarchically porous carbon foams for electric double layer capacitors.* Nano Research, 2016. **9**(10): p. 2875-2888.

[6]. Hao, P., et al., *Graphene-based nitrogen self-doped hierarchical porous carbon aerogels derived from chitosan for high performance supercapacitors.* Nano Energy, 2015. **15**: p. 9-23.

[7]. Hu, Y., et al., *Preparation of Chitosan-Based Activated Carbon and Its Electrochemical Performance for EDLC.* J ELECTROCHEM SOC, 2013. **160**(6): p. H321-H326.

[8]. Deng, X., et al., *Molten salt synthesis of nitrogen-doped carbon with hierarchical pore structures for use as high-performance electrodes in supercapacitors.* CARBON, 2015. **93**: p. 48-58.

[9]. Sun, L., et al., *Isolated boron and nitrogen sites on porous graphitic carbon synthesized from nitrogen-containing chitosan for supercapacitors.* Chemsuschem, 2014. **7**(6): p. 1637-1646.

[10]. Śliwak, A., et al., *Nitrogen-containing chitosan-based carbon as an electrode material for high-performance supercapacitors.* J.Appl Electrochem, 2016. **46**(6): p. 667-677.

[11]. Deng, J., et al., *Inspired by bread leavening: one-pot synthesis of hierarchically porous carbon for supercapacitors.* GREEN CHEM, 2015. **17**(7): p. 4053-4060.

[12]. Kucinska, A., A. Cyganiuk, and J.P. Lukaszewicz, *A microporous and high surface area active carbon obtained by the heat-treatment of chitosan.* Carbon, 2012. **50**(8): p. 3098-3101.

[13]. Jiang, Y., et al., *Controllable synthesis and capacitive performance of nitrogen-doped porous carbon from carboxymethyl chitosan by template carbonization method.* J SOLID STATE ELECTR, 2015. **19**(10): p. 3087-3096.

[14]. Zhu, L., et al., *High‐Performance Supercapacitor Electrode Materials from Chitosan via Hydrothermal Carbonization and Potassium Hydroxide Activation.* ENERGY TECHNOL, 2017. **5**.

[15]. Lota, K., et al., *The capacitance properties of activated carbon obtained from chitosan as the electrode material for electrochemical capacitors.* Mater Lett, 2016. **173**: p. 72-75.

[16]. Wei, L., et al., *Hydrothermal Carbonization of Abundant Renewable Natural Organic Chemicals for High‐Performance Supercapacitor Electrodes.* Adv.Energy Mater, 2011. **1**(3): p. 356-361.

[17]. Bai, S., et al., *Cover Picture: Pumpkin‐Derived Porous Carbon for Supercapacitors with High Performance (Chem. Asian J. 12/2016).* CHEM-

ASIAN J, 2016. **11**(12): p. 1828.
[18]. Ding, J., et al., *Peanut shell hybrid sodium ion capacitor with extreme energy–power rivals lithium ion capacitors.* ENERG ENVIRON SCI, 2015. **8**(3): p. 941-955.
[19]. Liu, X., et al., *Microtube bundle carbon derived from Paulownia sawdust for hybrid supercapacitor electrodes.* ACS APPL MATER INTER, 2013. **5**(11): p. 4667-4677.
[20]. Zhang, L., et al., *Interconnected Hierarchical Porous Carbon from Lignin-Derived Byproducts of Bioethanol Production for Ultra-High Performance Supercapacitors.* ACS Appl. Mat. Interfaces 2016. **8**(22): p. 13918.
[21]. Sevilla, M. and A.B. Fuertes, *Sustainable porous carbons with a superior performance for CO2 capture.* Energ Environ.SCI 2011. **4**(5): p. 1765-1771.
[22]. Pampel, J., C. Denton, and T.P. Fellinger, *Glucose derived ionothermal carbons with tailor-made porosity.* Carbon, 2016. **107**: p. 288-296.
[23]. Li, X., et al., *Preparation and performance of straw based activated carbon for supercapacitor in non-aqueous electrolytes.* Micropor Mesopor Mat, 2010. **131**(1): p. 303-309.
[24]. Olivares-Marín, M., et al., *Cherry stones as precursor of activated carbons for supercapacitors.* Mater Chem Phys, 2009. **114**(1): p. 323-327.
[25]. Kalpana, D., et al., *Recycled waste paper—A new source of raw material for electric double-layer capacitors.* J. Power Sources, 2009. **190**(2): p. 587-591.
[26]. Wang, H., et al., *Interconnected carbon nanosheets derived from hemp for ultrafast supercapacitors with high energy.* Acs Nano, 2013. **7**(6): p. 5131-5141.
[27]. Zhou, L., et al., *Naturally derived carbon nanofibers as sustainable electrocatalysts for microbial energy harvesting: A new application of spider silk.* APPL CATAL B-ENVIRON 2016. **188**: p. 31-38.
[28]. Wei, T., et al., *Large scale production of biomass-derived nitrogen-doped porous carbon materials for supercapacitors.* Electrochim Acta, 2015. **169**: p. 186-194.
[29]. Biswal, M., et al., *From dead leaves to high energy density supercapacitors.* ENERG ENVIRON SCI, 2013. **6**(4): p. 1249-1259.
[30]. Zhu, L., et al., *Black liquor-derived porous carbons from rice straw for high-performance supercapacitors.* Chem. Eng. J, 2017. **316**: p. 770-777.
[31]. Gao, F., et al., *Nitrogen-doped activated carbon derived from prawn shells for high-performance supercapacitors.* Electrochim Acta, 2016. **190**: p. 1134-1141.
[32]. Wei, J., et al., *A Controllable Synthesis of Rich Nitrogen‐Doped Ordered Mesoporous Carbon for CO2 Capture and Supercapacitors.* Adv.Funct Mater, 2013. **23**(18): p. 2322-2328.
[33]. Xie, L., et al., *Hierarchical Porous Carbon Microtubes Derived from Willow Catkins for Supercapacitor Application.* J. Mater Chem. A, 2015. **4**(5): p. 1637-1646.

[34]. Liu, Y., et al., *Biomass-derived hierarchical porous carbons: boosting the energy density of supercapacitors via an ionothermal approach.* J .Mater Chem. A, 2017. **5**(25).

[35]. Jiang, D., et al., *Inspired by bread leavening: one-pot synthesis of hierarchically porous carbon for supercapacitors.* Green Chem, 2015. **17**(7): p. 4053-4060.

[36]. Huang, Y., et al., *Biobased Nano Porous Active Carbon Fibers for High-Performance Supercapacitors.* ACS APPL MATER INTER, 2016. **8**(24): p. 15205-15215.

[37]. Wu, C., et al., *Activated Microporous Carbon Derived from Almond Shells for High Energy Density Asymmetric Supercapacitors.* ACS Appl. Mat. Interfaces, 2016. **8**(24): p. 15288.

[38]. Wang, C., et al., *Biomass derived nitrogen-doped hierarchical porous carbon sheets for supercapacitors with high performance.* J.Colloid Interf. Sci, 2018. **523**.

[39]. Thangavel, R., et al., *Engineering the Pores of Biomass‐Derived Carbon: Insights for Achieving Ultrahigh Stability at High Power in High‐Energy Supercapacitors.* Chemsuschem, 2017. **10**(13).

[40]. Li, Q., et al., *β‐Ni(OH)2 nanosheet arrays grown on biomass‐derived hollow carbon microtube for high‐performance asymmetric supercapacitor.* Chemelectrochem, 2018.

[41]. Chun, H.H., et al., *A Solvent-Free Synthesis of Lignin-Derived Renewable Carbon with Tunable Porosity for Supercapacitor Electrodes.* ChemSusChem. **0**(ja).

[42]. Jian, S., et al., *Hierarchical Porous Carbons Derived from Renewable Poplar Anthers for High-Performance Supercapacitors.* ChemElectroChem, 2018. **5**(11): p. 1451-1458.

[43]. Dengfeng, Y., et al., *Biowaste-Derived Hierarchical Porous Carbon Nanosheets for Ultrahigh Power Density Supercapacitors.* ChemSusChem, 2018. **11**(10): p. 1678-1685.

[44]. Wei, T., et al., *A one-step moderate-explosion assisted carbonization strategy to sulfur and nitrogen dual-doped porous carbon nanosheets derived from camellia petals for energy storage.* J.Power Sources, 2016. **331**: p. 373-381.

[45]. Yao, Y., et al., *Rational design of high-surface-area carbon nanotube/microporous carbon core-shell nanocomposites for supercapacitor electrodes.* ACS Appl. Mat. Interfaces 2015. **7**(8): p. 4817-4825.

[46]. Sun, F., et al., *High performance aqueous supercapacitor based on highly nitrogen-doped carbon nanospheres with unimodal mesoporosity.* J. Power Sources, 2017. **337**: p. 189-196.

[47]. Wen, L., et al., *Multiple nanostructures based on anodized aluminium oxide*

templates. Nat. Nanotechnol., 2016. **12**: p. 244.